ACCOUNTS
of chemical research

Carbide Cluster Metallofullerenes: Structure, Properties, and Possible Origin

XING LU,[*,†,‡] TAKESHI AKASAKA,[*,†,‡,§] AND SHIGERU NAGASE[∥]

[†]*State Key Laboratory of Material Processing and Die & Mould Technology, School of Materials Science and Engineering, Huazhong University of Science and Technology (HUST), Wuhan, Hubai 430074, China,* [‡]*Life Science Center of Tsukuba Advanced Research Alliance, University of Tsukuba, Tsukuba, Ibaraki 305-8577, Japan,* [§]*Foundation for Advancement of International Science, Tsukuba, Ibaraki 305-0821, Japan, and* [∥]*Fukui Institute for Fundamental Chemistry, Kyoto University, Sakyo-ku, Kyoto 606-8103, Japan*

RECEIVED ON JANUARY 13, 2013

CONSPECTUS

Endohedral metallofullerenes (EMFs) are hybrid molecules with different metallic species encapsulated inside the fullerene cages. In addition to conventional EMFs that contain only metal ions, researchers have constructed novel compounds that encapsulate metallic clusters of nitride, carbide, oxide, cyanide, and sulfide. Among these structures, carbide cluster metallofullerenes (CCMFs) are unique because their synthesis requires only graphite and the metal source. As a result the molecular structures of CCMFs are particularly difficult to characterize. Two carbon atoms are encapsulated inside the cage, but they do not participate in constructing the cage framework. Recent X-ray crystallographic studies of EMFs have allowed researchers to unambiguously identify CCMFs ($M_xC_2@C_{2n}$). Previously most of these structures had been described as conventional EMFs $M_x@C_{2n+2}$. Most of these species are scandium-containing compounds such as $Sc_3C_2@I_h(7)$-C_{80} [not $Sc_3@C_{3v}(7)$-C_{82}], $Sc_2C_2@C_{2v}(5)$-C_{80} [not $Sc_2@C_{82}$], $Sc_2C_2@C_s$-(6)-C_{82} [not $Sc_2@C_s(10)$-C_{84}], $Sc_2C_2@C_{2v}(9)$-C_{82} [not $Sc_2@C_{2v}(17)$-C_{84}], $Sc_2C_2@C_{3v}(8)$-C_{82} [not $Sc_2@D_{2d}(23)$-C_{84}], and $Sc_2C_2@D_{2d}(23)$-C_{84} [not $Sc_2@C_{86}$]. Additional examples of CCMFs include $Gd_2C_2@D_3(85)$-C_{92}, $Sc_2C_2@C_{2v}(6073)$-C_{68}, $Ti_2C_2@D_{3h}(5)$-C_{78}, $M_2C_2@C_{3v}(8)$-C_{82}, $M_2C_2@C_s(6)$-C_{82} (M = Y, Er, etc.), $Y_2C_2@C_{84}$, $Y_2C_2@D_3(85)$-C_{92}, $Y_2C_2@D_5(450)$-C_{100}, and $Lu_3C_2@D_2(35)$-C_{88}. The existence of so many CCMF species reminds us that the symbol `@' (which denotes the encapsulation status of EMFs) should be used with caution with species whose molecular structures have not been determined unambiguously.

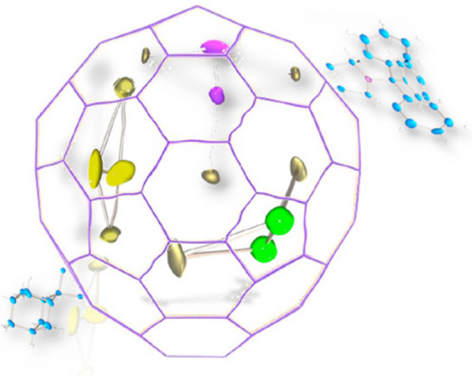

This Account presents a detailed summary of all aspects of CCMFs, including historically erroneous assignments and corrected structural characterizations, along with their intrinsic properties such as electrochemical and chemical properties. We emphasize structural issues, features that are fundamental for understanding their intrinsic properties. Finally, we discuss the formation mechanism and possible origin of cluster EMFs, not just CCMFs.

1. Introduction

Fullerenes are the only soluble carbon allotrope with definite molecular structures.[1] These features are fundamentally important for accurate elucidation of their molecular structures and for in-depth understanding of their inherent properties. Relevant results are also helpful to enhance our knowledge of their formation mechanisms and intrinsic properties of the related carbon materials such as carbon nanotubes and graphene, sequentially enabling improvement of their production efficiency and ultimately realizing their wide application.[2]

The unique structure of fullerenes provides a novel platform for additional derivatization, either by attaching different functional groups to the surface[3] or by replacing a cage carbon with a heteroatom, thereby affording heterofullerenes.[4] More intriguingly, the interior of the

Published on the Web 05/01/2013 www.pubs.acs.org/accounts
10.1021/ar4000086

fullerenes can encapsulate various atoms, clusters, and molecules, thereby forming endofullerenes.[5] When metallic species are encapsulated, the resultant endohedral metallofullerenes (EMFs) are attractive because intramolecular electron transfer from the internal metallic species to the fullerene cage takes place, which makes EMFs different from empty fullerenes.[6]

Presently, the most effective means for EMF production is the so-called direct-current arc discharge method, which has shown great success in producing EMFs of many kinds.[7] Conventional EMFs are species encapsulating purely metal ions ($M_x@C_{2n}$), whereas novel EMFs contain a metallic cluster of various kinds; they are also called cluster EMFs.[8] The first recognized cluster EMF was $Sc_3N@C_{80}$, obtained by accidental leakage of nitrogen into the discharge chamber.[9] Other cluster-EMFs containing clusters of metal oxide, sulfide, and even cyanide were synthesized similarly by adding corresponding heterogeneous additives into the reactor.[10]

Carbide cluster metallofullerenes (CCMFs) were also obtained, but their formation requires no extra component other than graphite and the metal sources. As a direct result, CCMFs are hardly distinguishable from conventional EMFs in view of their structural features. Indeed, many CCMFs were assigned erroneously as di-EMFs or tri-EMFs. During the past decade, CCMFs have been discovered with increasing frequency, and their structures have been established concretely. Regarding the intractable structural issues and the largely unexplored properties of CCMFs, we herein give an Account addressing all important achievements related to CCMFs, hoping to attract more interest from multiple disciplines of sciences that might finally clarify the many mysteries currently existing in the research of EMFs.

2. Structure of CCMFs

2.1. Characterization Methods: A Comparison. Structural elucidation of EMFs has persisted as an important research task because their intrinsic properties are associated closely with these structural issues. Several techniques have been used to determine EMF structures.

2.1.1. Synchrotron Radiation Powder Diffraction/Rietveld Analysis/Maximum Entropy Method (SRPD/Rietveld/MEM). This technique provided the first experimental evidence for the endohedral nature of EMFs.[11] The first CCMF species, $Sc_2C_2@D_{2d}(23)$-C_{84}, was also discovered using this method along with nuclear magnetic resonance (NMR) study.[12] However, this method is not always reliable for providing accurate information related to the cage structures and metal positions of EMFs, most probably because of the arbitrary data treatment process. Furthermore, the high cost of the facilities limits their wide application.

2.1.2. Nuclear Magnetic Resonance (NMR) Spectroscopy. The carbon-rich composition of fullerenes and EMFs is beneficial for ^{13}C NMR investigation, which has shown great success in establishing the cage symmetry of many fullerene/EMF species. For uncertain metal locations, a metal nuclei NMR technique sometimes validates the estimation of the dynamic metal motion. Some meaningful results have been reported.[13]

2.1.3. Single-Crystal X-ray Diffraction (XRD) Crystallography. This more reliable method invariably requires high-quality single crystals and professional data-treatment skills. Practically speaking, samples with sufficient order suitable for X-ray analyses are obtainable either by cocrystal formation with countering molecules such as metal porphyrin or by covalent exohedral modification with different kinds of functional groups. Both show great success in hindering the rotation of the fullerene/EMF molecules in the crystal units. Many examples have been reported during recent years.[6]

2.1.4. Theoretical Calculations. Computational works can provide additional evidence related to the structures and properties of EMFs beyond the ability of experimental techniques. For instance, the amount of electrons transferred from metal to cage in a given EMF compound can be estimated theoretically, but it is not an experimentally measurable quantity. Recent computational works have specifically examined the stability, formation mechanism, and metal−cage interactions of typical EMFs including CCMFs; the results have greatly enhanced our knowledge of these novel metal−carbon hybrid molecules.[14]

2.2. Scandium-Based CCMFs. EMFs containing Sc-only ion(s) or Sc-only clusters are generally more abundant than those containing other metal elements. In fact, only scandium is reported to form all kinds of the EMFs obtained to date. As a result, isolated examples of Sc-based CCMFs are far more numerous than others, and accordingly, they are better understood.[15]

2.2.1. $Sc_2C_2@D_{2d}(23)$-C_{84}. This is the first structurally identified CCMF compound. Its ^{13}C NMR pattern [10×8, 1×4] directly pointed to the $D_{2d}(23)$-C_{84} cage rather than any C_{86} isomer.[12] A recent NMR study with a ^{13}C-enriched sample detected the C_2-signal at 249.2 ppm, which agrees perfectly with the calculated value (279.3 ppm).[16] X-ray crystallographic study of $Sc_2C_2@D_{2d}(23)$-C_{84}/2Co(OEP) (OEP is 2,3,7,8,12,13,17,18-octaethylporphinate)

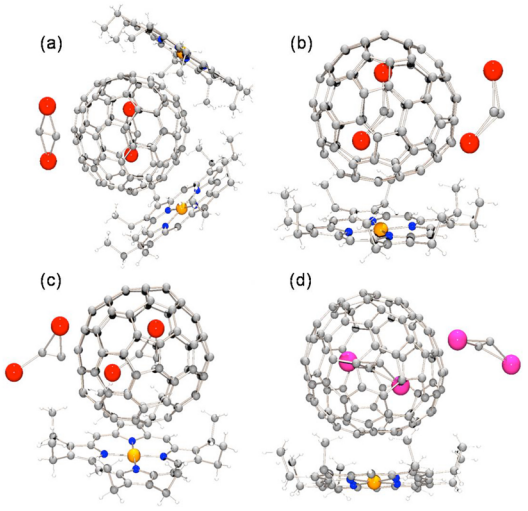

FIGURE 1. Structures of typical CCMFs cocrystallized with M(OEP) (M = Ni or Co): (a) Sc_2C_2@D_{2d}(23)-C_{84}/2Co(OEP); (b) Sc_2C_2@C_{3v}(8)-C_{82}/Co(OEP); (c) Sc_2C_2@C_{2v}(5)-C_{80}/Co(OEP); (d) Gd_2C_2@D_3(85)-C_{92}/Ni(OEP). C, gray; N, blue; Sc, red; Gd, pink; Co/Ni, orange. The encapsulated carbide cluster in each compound is displayed separately to enhance visualization.

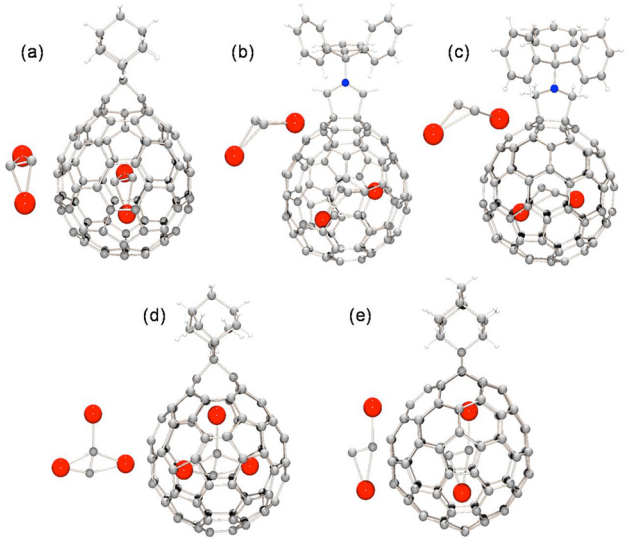

FIGURE 2. Structures of representative derivatives of Sc-based CCMFs: (a) Sc_2C_2@C_{3v}(8)-C_{82}Ad; (b) Sc_2C_2@C_s(6)-$C_{82}(CH_2)_2$NTrt; (c) Sc_2C_2@C_{2v}(9)-$C_{82}(CH_2)_2$NTrt; (d) Sc_3C_2@I_h(9)-C_{80}Ad; (e) Sc_2C_2@C_{2v}(5)-C_{80}Ad. C, gray; N, blue; Sc, red. The encapsulated carbide cluster in each compound is displayed separately to enhance visualization.

cocrystals suggests that Sc_2C_2 is bent with a Sc−C_2−Sc dihedral angle of 154.3° (Figure 1a).[17]

2.2.2. Sc_2C_2@C_s(6)-C_{82}, Sc_2C_2@C_{3v}(8)-C_{82}, and Sc_2C_2@C_{2v}(9)-C_{82}. In 2000, a systematic ^{13}C NMR study of the three Sc_2C_{84} isomers proposed that they were conventional EMFs Sc_2@C_s(10)-C_{84}, Sc_2@C_{2v}(17)-C_{84}, and Sc_2@D_{2d}(23)-C_{84} for isomers Sc_2C_{84}-I, -II, and -III, respectively.[18] However, recent results confirmed that all of them are CCMFs. First, Sc_2@D_{2d}(23)-C_{84} was revealed to be Sc_2C_2@C_{3v}(8)-C_{82} by NMR spectroscopy with the C_2-signal being observed at 253.2 ppm.[16,19] X-ray crystallographic results of either Sc_2C_2@C_{3v}(8)-C_{82}/Co(OEP) cocrystals (Figure 1b) or its carbene adduct (Figure 2a) confirmed a butterfly-like cluster configuration.[17] Similarly, ^{13}C NMR studies of the other two Sc_2C_{84} isomers firmly established their correct structures as Sc_2C_2@C_s(6)-C_{82} and Sc_2C_2@C_{2v}(9)-C_{82}, respectively.[20,21] The bent structure of the internal Sc_2C_2 clusters in both compounds was established further using XRD crystallography performed on their pyrrolidino-derivatives (Figure 2b,c).

Because all Sc_2C_{84} isomers have now been verified as CCMF species, previous results related to the erroneous Sc_2@C_{84} structures are patently inaccurate. They must be re-examined. For example, high-resolution TEM images of the "Sc_2@C_{84}" molecules inside single-wall carbon nanotubes have also observed the bent structure of the internal metallic species, and the two encapsulated carbon atoms also project shadows in the simulated HR-TEM images. Unfortunately, the authors did not realize that these molecules are actually CCMFs.[22]

2.2.3. Sc_3C_2@I_h-C_{80}. First isolated in 1994, Sc_3C_{82} was proposed as $[Sc_3]^{3+}$@$[C_{3v}(7)\text{-}C_{82}]^{3-}$ with SRPD/Rietveld/MEM in 1999.[23] However, in 2005, ^{13}C NMR studies performed on its monoanion excluded the possibility of any C_{82} cage but pointed to the icosahedral C_{80}.[24] Observation of the C_2-signal from the endohedral entity at 328.3 ppm further corroborated its molecular structure as Sc_3C_2@I_h-C_{80}, and X-ray results of its carbene derivative revealed a planar Sc_3C_2 cluster with the central C_2-moiety surrounded by three scandium ions (Figure 2d).

Sc_4C_2@I_h-C_{80} was also obtained.[25] The I_h-C_{80} cage structure was established by ^{13}C NMR spectroscopy, and for the cluster configuration, DFT calculations proposed that the C_2-unit is trapped inside the vacancy formed by four Sc^{3+} ions. FT-IR and Raman spectroscopic results also supported the matryoshka-like structure. Furthermore, the ^{13}C NMR chemical shift values of the internal cluster were computed as 226.1 and 326.7 ppm but were not observed experimentally, probably because of the spin-rotation interaction and the low signal-to-noise ratio.

2.2.4. Sc_2C_2@C_{2v}(5)-C_{80}. In 1999, two Sc_2C_{82} isomers were isolated from soot extract, but they were not determined structurally. A recent NMR study of Sc_2C_{82}(I) revealed its carbide structure as Sc_2C_2@C_{2v}(5)-C_{80}.[26] The signal from the C_2-moiety is readily detected at 231.5 ppm. X-ray results

of its cocrystal with Co(OEP) confirmed that the Sc_2C_2 cluster is also bent with a Sc−C_2−Sc dihedral angle of about 131° (Figure 1c).[17] Another X-ray study of its carbene derivative found that the cluster is less deformed than in the pristine compound because of cage opening (Figure 2e).[27]

Variable-temperature NMR studies of Sc_2C_2@C_{2v}(5)-C_{80} revealed that the internal cluster is fixed inside the cage at a temperature below 373 K, reducing the molecular symmetry from C_{2v} to C_s, although it rotates upon increasing temperatures, expressing negligible influences on the cage carbons. Similar results were also observed for Sc_2C_2@C_s(6)-C_{82} and Sc_2C_2@C_{2v}(9)-C_{82}. Accordingly, such a temperature-sensitive dynamic motion of the internal Sc_2C_2 cluster can be regarded as a characteristic feature of CCMFs.

2.2.5. Sc_2C_2@C_s(6073)-C_{68}. DFT interpretation of the preliminary NMR results suggests that this compound uses a fullerene cage that violates the isolated pentagon rule (IPR) with two pairs of fused pentagons, each closely approaching a Sc^{3+} ion.[28] However, a recent computational argument holds that the non-IPR Sc_2@C_{2v}(7854)-C_{70}, which bears three pairs of fused pentagons, should be more stable and also

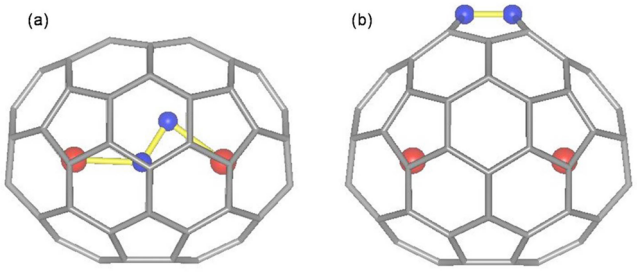

FIGURE 3. Optimized structures of (a) Sc_2C_2@C_s(6073)-C_{68} and (b) Sc_2@C_{2v}(7854)-C_{70}, showing their structural similarities.

that it reasonably fits the NMR spectrum.[29] Consequently, X-ray results are highly desired to resolve the controversy. Actually, these two cages are mutually similar to a great degree, as portrayed in Figure 3.

Examples of CCMFs containing a scandium carbide cluster (Sc_2C_2, Sc_3C_2, or Sc_4C_2) reported to date are presented collectively in Table 1. Because many Sc-EMFs have not been fully characterized, it is anticipated that more Sc-based CCMFs will be discovered in the near future.

2.3. CCMFs Containing Other Metals. In 2004, three Y_2C_2@C_{82} isomers were characterized with NMR spectroscopy as Y_2C_2@C_{3v}(8)-C_{82}, Y_2C_2@C_s(6)-C_{82}, and Y_2C_2@C_{2v}(9)-C_{82}. Existence of the three Y_2@C_{82} isomers having the same cages indicates a C_2-loss/C_2-encapsulation mechanism for EMF formation.[32] An abnormal pentagonal dodecahedron conformation of the Y_2C_2 moiety in Y_2C_2@C_{3v}(8)-C_{82} was deduced further from the SRPD/Rietveld/MEM results, which also indicated that nearly six electrons are transferred from the cluster to the cage.

Recently, Dorn and co-workers reported a systematic experimental and computational NMR study of a series of Y_2C_2@C_{2n} (n = 41, 42, 46, 50) isomers.[33] They found that the internal Y_2C_2 cluster tends to adopt a nearly linear structure when the cage is sufficiently large (e.g., C_{100}), although it is bent in smaller cages (C_{82}, C_{84}), like a butterfly. This results from a "nanoscale compression effect" of the fullerene cage on the internal yttrium carbide cluster, as shown schematically in Figure 4. No other example of Y-based CCMFs has been reported.

Similarly, three isomers containing an Er_2C_2 cluster were identified as Er_2C_2@C_s(6)-C_{82}, Er_2C_2@C_{3v}(8)-C_{82}, or Er_2C_2@C_{2v}(9)-C_{82} based on their spectral similarities to

TABLE 1. Structurally Identified CCMFs

compound	alias	associated characterizations[a]	C_2-signal, ppm	refs
Sc_2C_2@C_{2v}(6073)-C_{68}	Sc_2@C_{2v}(7854)-C_{70}	MS, UV, ^{13}C NMR, QC		28
Sc_2C_2@C_{2v}(5)-C_{80}	Sc_2@C_{82} (II)	MS, UV, ^{13}C NMR, QC	231.5	17,26
Sc_3C_2@I_h(7)-C_{80}	Sc_3@C_{3v}(7)-C_{82}	MS, UV, NMR, QC	328.3 (anion)	24
Sc_4C_2@I_h(7)-C_{80}		MS, UV, ^{13}C NMR, QC		25
Sc_2C_2@C_s(6)-C_{82}	Sc_2@C_s(10)-C_{84}	MS, UV, ^{13}C NMR, QC, XRD-der	244.4	20
Sc_2C_2@C_{3v}(8)-C_{82}	Sc_2@D_{2d}(23)-C_{84}	MS, UV, ^{13}C NMR, QC, XRD-der/Co(OEP)	253.2	16,19,30
Sc_2C_2@C_{2v}(9)-C_{82}	Sc_2@C_{2v}(17)-C_{84}	MS, UV, ^{13}C NMR, QC, XRD-der	242.7	21
Sc_2C_2@D_{2d}(23)-C_{84}	Sc_2@C_{86}	MS, UV, ^{13}C NMR, QC, XRD-der/XRD-Co(OEP)	249.2	12,17
Ti_2C_2@D_{3h}(5)-C_{78}	Ti_2@I_h(7)-C_{80} and Ti_2@D_{5h}(6)-C_{80}	MS, UV, EELS, QC	(288.5)	31
Y_2C_2@C_s(6)-C_{82}		MS, UV, QC	256.2	32
Y_2C_2@C_{3v}(8)-C_{82}		MS, UV, QC	257.0 (288)	
Y_2C_2@C_{2v}(9)-C_{82}		MS, UV, QC		
Y_2C_2@D_3(85)-C_{92}		^{13}C NMR	227.3 (229)	33
Y_2C_2@D_5(450)-C_{100}		QC	(156)	
Y_2C_2@ C_{84}		HPLC, MS	247.8	
Lu_3C_2@D_2 (35)-C_{88}		MS, UV, QC		34

[a]MS = mass spectrometry; UV = UV-vis-NIR spectrometry; NMR = nuclear magnetic resonance; QC = quantum computation; XRD-der = X-ray diffraction crystallography of derivatives; XRD-Co(OEP) = X-ray diffraction crystallographic study of cocrystals with metal porphyrin.

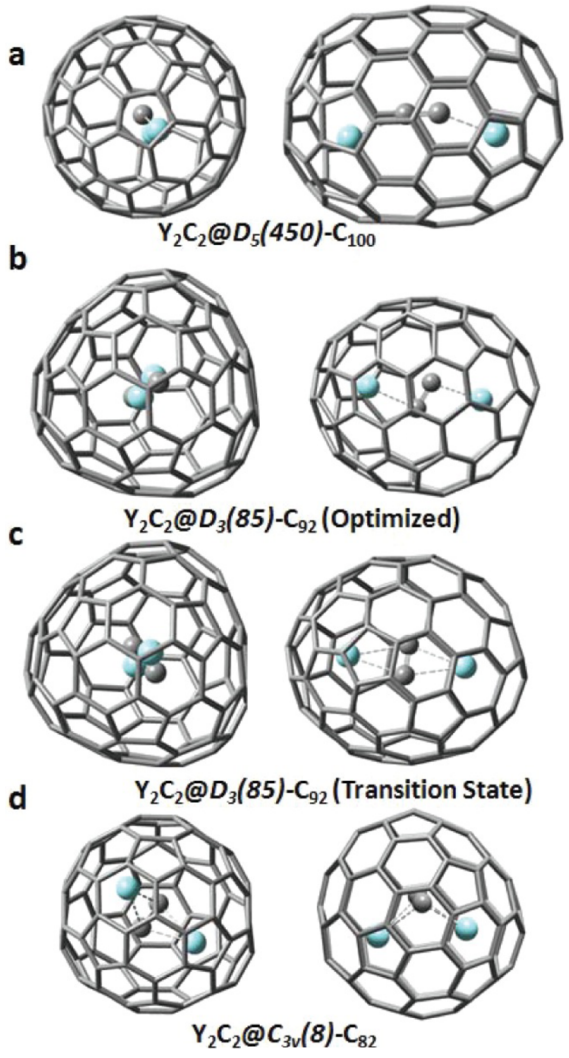

FIGURE 4. Nanoscale compression of an Y_2C_2 cluster by different fullerene cages: (a) optimized $Y_2C_2@D_5(8)$-C_{100}; (b) optimized $Y_2C_2@D_3(85)$-C_{92}; (c) transition state of $Y_2C_2@D_3(85)$-C_{92}; (d) optimized $Y_2C_2@C_{3v}(450)$-C_{100}. Reproduced from ref 33 with permission. Copyright 2012 American Chemical Society.

those of the respective $Y@C_{82}$ isomers. Their photoluminescence (PL) properties were also investigated together with these $Er_2@C_{82}$ isomers bearing the same cage structures to evaluate the influences of both the fullerene cage and the internal cluster. Results showed that the PL intensities depend sensitively on the cage symmetry, correlating strongly with absorbance at 1520 nm where Er^{3+} emits and the HOMO−LUMO energy gap of the molecules, which can be widened upon C_2-encapsulation.[35]

$Gd_2C_2@D_3(85)$-C_{92} bears the largest cage found to date for CCMFs. X-ray crystallography unambiguously established its molecular structure (Figure 1d). It was revealed that the butterfly-like Gd_2C_2 cluster is flatter than that of Sc_2C_2 in $Sc_2C_2@C_{2n}$ ($2n = 80-84$) and that the two Gd^{3+} ions move independently relative to the cage and the C_2-moiety.[36]

The previously proposed $Ti_2@C_{80}$ isomers were later confirmed by computational studies as a new CCMF $Ti_2C_2@D_{3h}(5)$-C_{78}, based on the reported NMR spectrum (Table 1). The NMR signal of the two equivalent acetylide carbon atoms of Ti_2C_2 was calculated as 288.5 ppm, which is in line with the experimental values of the corresponding Sc-containing and Y-containing CCMFs.[31]

Another trimetallic carbide cluster EMF following the better-studied $Sc_3C_2@I_h$-C_{80} is $Lu_3C_2@D_2(35)$-C_{88}. Its structure was deduced tentatively from absorption spectroscopy and Raman spectrometry. DFT calculations proposed a planar cluster configuration, resembling the Sc_3C_2 found in $Sc_3C_2@I_h$-C_{80}. An electronic structure of $(Lu_3C_2)^{6+}@D_2(35)$-$(C_{88})^{6-}$ was also proposed assuming that the unpaired electron localizes on the cluster rather than on the cage orbital.[34]

3. Electrochemical and Chemical Properties of CCMFs

3.1. Redox Behaviors of CCMFs. Electrochemical investigations of CCMFs have mainly examined such compounds containing a Sc_xC_2 ($x = 2$, 3, or 4) cluster, as well as their derivatives, while other CCMF species have not been studied intensively.

Redox potentials of typical CCMFs and their derivatives are presented in Table 2. In general, such CCMFs containing a Sc_2C_2 cluster normally display one oxidation step and two or three reversible reduction processes, with an electrochemical bandgap larger than 1.0 V, indicative of a closed-shell electronic configuration. It is noteworthy that $Sc_4C_2@I_h(7)$-C_{80} has the largest bandgap value among all Sc-based CCMFs, which is not only attributable to its closed-shell structure but also resulted from a size-matching stabilization effect between the internal cluster and the cage.[25]

Exceptionally small electrochemical bandgap values (0.44 and 0.47 V, respectively) are observed for $Sc_3C_2@I_h$-C_{82} and its carbene derivative [$Sc_3C_2@I_h(7)$-C_{80}Ad], each exhibiting one reversible oxidation step and three reversible reduction processes.[24] It is now acknowledged that the small bandgaps are attributable to their open-shell electronic configurations. In contrast, the other trimetallic carbide CCMF compound, $Lu_3C_2@D_2(35)$-C_{88}, features the largest bandgap value (1.65 V) among all studied CCMFs, implying a closed-shell electronic configuration.[34]

Chemical modification of CCMFs can influence their electrochemical properties to a certain degree. For example, the

TABLE 2. Redox Potentials (V vs Fc/Fc^+) of Typical CCMFs and Their Derivatives

compound	$^{ox}E_1$	$^{red}E_1$	$^{red}E_2$	$^{red}E_3$	ΔE ($^{ox}E_1 - {}^{red}E_1$)	ref
C_{60}	1.21	−1.12	−1.50	−1.95	2.33	37
$Sc_2C_2@C_{2v}(5)$-C_{80}	0.41	−0.74	−1.33		1.15	26
$Sc_2C_2@C_{2v}(5)$-C_{80}Ad-A	0.14	−0.96	−1.69		1.10	27
$Sc_2C_2@C_{2v}(5)$-C_{80}Ad-B	0.28	−0.87	−1.56		1.15	
$Sc_2C_2@C_{2v}(5)$-C_{80}Ad-C	0.27	−0.89	−1.48		1.16	
$Sc_2C_2@C_{2v}(5)$-C_{80}Ad-D	0.28	−0.86	−1.53		1.14	
$Sc_2C_2@C_{2v}(5)$-C_{80}Ad-E	0.11	−0.75	−1.46		0.86	
$Sc_3C_2@I_h(7)$-C_{80}	−0.11	−0.55	−1.74	−1.84	0.44	24
$Sc_3C_2@I_h(7)$-C_{80}Ad	−0.03	−0.50	−1.64	−1.84	0.47	
$Sc_4C_2@I_h(7)$-C_{80}	0.40	−1.16	−1.65		1.56	25
$Sc_2C_2@C_s(6)$-C_{82}	0.64	0.42	−0.93	−1.30	1.35	20
$Sc_2C_2@C_s(6)$-$C_{82}(CH_2)_2$NTrt	0.65	0.33	−1.25	−1.60	1.58	
$Sc_2C_2@C_{3v}(8)$-C_{82}	0.47	−0.94	−1.15	−1.60	1.41	30
$Sc_2C_2@C_{3v}(8)$-C_{82}Ad	0.38	−0.79	−1.12	−1.63	1.17	
$Sc_2C_2@C_{2v}(9)$-C_{82}	0.67	0.25	−0.74	−0.96	0.99	21
$Sc_2C_2@C_{2v}(9)$-$C_{82}(CH_2)_2$NTrt-A	0.70	0.27	−1.13	−1.56	1.40	
$Sc_2C_2@C_{2v}(9)$-$C_{82}(CH_2)_2$NTrt-B	0.73	0.39	−0.84	−1.19	1.23	
$Sc_2C_2@C_{2v}(9)$-$C_{82}(CH_2)_2$NTrt-C	0.51	0.12	−1.07	−1.62	1.19	
$Lu_3C_2@D_2(35)$-C_{88}	0.31	−1.34	−1.70	−2.15	1.65	34

redox potentials of the Ad adducts of $Sc_2C_2@C_{2v}(5)$-C_{80} are normally more negative than the corresponding values of pristine $Sc_2C_2@C_{2v}(5)$-C_{80}, indicating an electron-donating ability of Ad.[27] The reduction peaks of the pyrrolidino derivatives of $Sc_2C_2@C_{82}$ are all more negative, but the oxidation processes are cathodically shifted, resulting in much larger electrochemical bandgaps for the derivatives. Consequently, it is acknowledged that chemical functionalization is an effective means to alter the properties of EMFs.[20,21]

3.2. Chemical Reactions. 3.2.1. Carbene Addition. Chemical behaviors of CCMFs have not been widely studied. An early reaction used to modify CCMFs is the cycloaddition of 2-adamantane-2,3-[3*H*]-diazirine (AdN_2), which generates adamantylidine carbene under heating or upon photoirradiation (Scheme 1). It is noteworthy that the resulting derivatives are more suitable than pristine EMFs for single-crystal growth to ascertain their molecular structures using X-ray crystallography.[38]

$Sc_3C_2@I_h$-C_{80} was first involved in this reaction. A monoadduct isomer was fully characterized. ^{13}C NMR study observed two signals for the encapsulated C_2-unit at 257.2 and 384.4 ppm, indicating two nonequivalent carbon atoms inside the cage.[16] X-ray results confirmed that the planar Sc_3C_2 cluster is fixed because one Sc atom is trapped inside the cavity provided by bond-breaking (Figure 2d).[24] This reaction was also performed on $Sc_2C_2@C_{3v}(8)$-C_{82} and the most abundant isomer was isolated and characterized with a series of experimental techniques. The Ad group adds to a [5,6]-bond junction that is far from either Sc ion (Figure 2a).[30]

The reaction of $Sc_2C_2@C_{2v}(5)$-C_{80} with AdN_2 has been described in greater detail.[27] Five monoadduct isomers were isolated, and the four most abundant adducts were structurally characterized with X-ray crystallography. Results showed that the Ad group tends to add to either a [5,6]- or a [6,6]-bond junction that are all distant from the Sc^{3+} ions. This unique addition pattern conflicts with the existing knowledge that the cage parts close to the internal metal ions are always more negatively charged and more pyramidalized to bear higher reactivity toward **1**.[39] Additional investigations must be undertaken to clarify this discrepancy.

SCHEME 1. Reactions That Have Been Performed on CCMFs

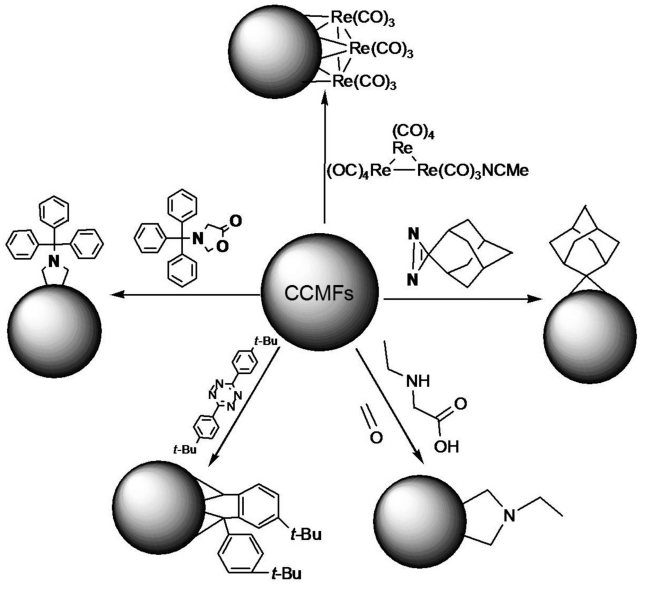

3.2.2. 1,3-Dipolar Reaction. Heating of 3-triphenylmethyl-5-oxazolidinone produces the corresponding 1,3-dipolar reagent that reacts with fullerenes or EMFs to afford

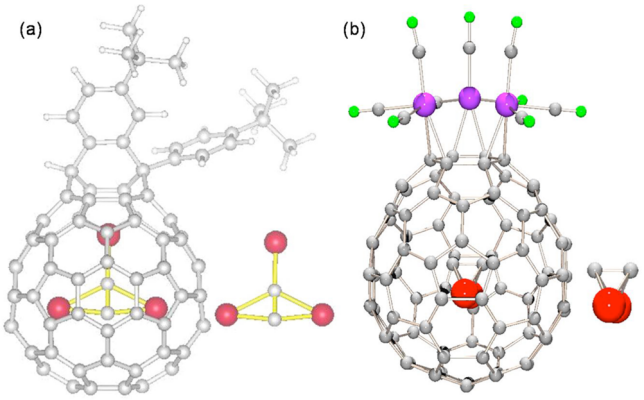

FIGURE 5. Structures of (a) bisfulleroid $Sc_3C_2@I_h$-$C_{80}C_{22}H_{26}$ and (b) $Sc_2C_2@C_{3v}(8)$-$C_{82}(\mu$-H$)_3Re_3(CO)_9$. The encapsulated carbide cluster of each compound is displayed separately to enhance visualization.

pyrrolidino-ring-fused derivatives. $Sc_2C_2@C_s(6)$-C_{82} and $Sc_2C_2@C_{2v}(9)$-C_{82} were both involved in this reaction (Scheme 1). Although $Sc_2C_2@C_s(6)$-C_{82} has as many as 44 nonequivalent cage carbons, and in principle, it is expected to produce many regioisomers, only one monoadduct isomer was formed in the reaction.[20] In contrast, the more symmetric $Sc_2C_2@C_{2v}(9)$-C_{82} gave rise to three isomers.[21] Based on concrete X-ray results of the corresponding adducts, computational works have revealed that the addition patterns in these CCMFs can be interpreted reasonably with the frontier molecular orbital theory by simply considering the LUMO distribution on the cage.

$Sc_3C_2@I_h$-C_{80} was also allowed to react with azomethine ylide to provide the corresponding fulleropyrrolidine (Scheme 1).[40] NMR results confirmed that the addition takes place at a [5,6]-bond junction. DFT calculations proposed that the nearly planar Sc_3C_2 cluster is fixed inside the cage that produces two sets of ESR signals from the nonequivalent Sc^{3+} nuclei, whereas three Sc^{3+} ions are homogeneous in pristine $Sc_3C_2@I_h$-C_{80}.

3.2.3. Miscellaneous Reactions. A bisfulleroid derivative of $Sc_3C_2@I_h$-C_{80} was obtained by cycloaddition of a substituted tetrazine, which had been adopted to construct a four-membered ring into the framework of C_{60}, forming a stable C_{62}-derivative (Scheme 1). A series of NMR characterizations revealed that the derivative of $Sc_3C_2@I_h$-C_{80} bears large orifices consisting of an octagon and two heptagons. Its optimized structure (Figure 5a) shows that the cluster is nearly fixed inside the cage, in line with ESR results.[41] The formation of a fulleroid derivative instead of a C_2-inserted adduct for $Sc_3C_2@I_h$-C_{80} was assumed to have resulted from its flatter cage surface than that of C_{60}.

The reaction between $Sc_2C_2@C_{3v}(8)$-C_{82} and $(\mu$-H$)_3Re_3(CO)_{11}$-NCMe afforded an air-stable compound, which represented the first example of a metal complex of EMFs.[42] X-ray results revealed a face-capping structure with the $(\mu$-H$)_3Re_3(CO)_9$ cluster coordinating to a unique hexagon that is perpendicular to the symmetric axis of the cage (Figure 5b). Although the electronic structure of $Sc_2C_2@C_{3v}(8)$-C_{82} has been changed upon complexation, no communication between the internal Sc_2C_2 cluster and the *exo* Re_3 cluster was observed.

4. Possible origin of Cluster EMFs

A persistent mystery is that the cluster involved in CCMFs invariably consists of two carbon atoms and some varying number of metal ions. This phenomenon coincidentally agrees with the recently proposed C_2-loss formation mechanism of fullerenes and EMFs.[43]

What is perhaps more interesting is that a clear correlation between the inherent properties of the encapsulated metal ions, such as the ionic radius, the valence state, and coordination ability, and the ease of forming cluster EMFs has been deduced from the many CCMFs with definite molecular structures. First, for highly coordinative rare earth metals, the small Sc^{3+}, Y^{3+}, and Lu^{3+} more prefer to form cluster EMFs, while large ions such as La^{3+}, Ce^{3+}, and Pr^{3+} do not form cluster EMFs efficiently.[44] Probably because of its small ionic radius, only scandium can form such large clusters as Sc_4C_2, Sc_3N, and Sc_4O_3 when imprisoned in these small cages between C_{68} and C_{80}. The detection of $Gd_2C_2@D_3(85)$-C_{92} shows that a large cluster demands a large cage to accommodate it. Consequently, it is anticipated that CCMFs containing, for example, La_2C_2, can be found in such large cages as C_{100} or larger. Furthermore, no example of cluster EMFs (not only CCMFs) has been confirmed to involve a divalent metal ion such as Ca^{2+} or Yb^{2+}. This fact suggests that the valence state of the metal ions, which is closely associated with their coordination abilities, is a critical factor in determining cluster formation.

5. Conclusion and Perspective

Following the intriguing nitride cluster EMF analogues, CCMFs have become the second largest sub-branch of cluster EMFs. Difficulties in the elucidation of CCMF structure because of the homogeneous composition of the C_2-unit and the pure-carbon cage have been circumvented to a great degree by X-ray crystallography. NMR techniques have also succeeded in detecting the signals of the encapsulated C_2-unit, although ^{13}C-enriched samples are normally

necessary, which simplifies the structural assignment of CCMFs. It is anticipated that future structural determinations of CCMFs will help to elucidate the EMF formation processes.

However, the availability of CCMFs is much less than sufficient for exploring their intrinsic properties. Moreover, knowledge of their chemistry remains in early infancy. Many possible chemical transformations await detailed exploration. Along with anticipated breakthroughs in knowledge of this field, applicable materials based on CCMFs will be obtained in the near future.

This work was supported by NSFC (Grant 21171061), The National Thousand Talents Program of China, HUST, KAKENHI (Grants 20108001, "pi-Space", 202455006, 24350019, 20036008 20038007, and 22000009), The Next Generation Super Computing Project (Nanoscience) from MEXT Japan, and The Strategic Japanese–Spanish Cooperative Program funded by JST & MICINN.

BIOGRAPHICAL INFORMATION

Xing Lu is a Professor in Huazhong University of Science and Technology supported by the National Thousand Talents Program of China, interested in rational design and facile production of novel hybrid carbon materials with applications in energy storage/conversion and biology. Born in 1975, he received his Ph.D. from Peking University in 2004. Subsequently, he worked as a COE Postdoctoral Fellow at Nagoya University. During 2006–2011, he was a Senior Scientist at the University of Tsukuba. He is the recipient of the Ambassador Award from the Chinese Embassy in Japan (2009) and The Osawa Award from the Fullerenes and Nanotubes Research Society of Japan (2011).

Takeshi Akasaka was born in Kyoto and grew up in Osaka, Japan. He received a Ph.D. degree from the University of Tsukuba in 1979. After working as a Postdoctoral Fellow at Brookhaven National Laboratory, he returned to the University of Tsukuba in 1981. In 1996, he moved to Niigata University as a Professor. Since 2001, he has been a Professor of the TARA Center and Department of Chemistry, University of Tsukuba. His research interests include the chemistry of nanocarbons. He received The Commendation for Science and Technology (Research Category) from The Ministry of Education, Culture, Sports, Science and Technology of Japan (2011) and The Chemical Society of Japan Award for Creative Work (2001).

Shigeru Nagase received a Ph.D. degree from Osaka University in 1975. After working as a postdoctoral fellow (1976–1979) at the University of Rochester and The Ohio State University, he returned to the Institute for Molecular Science in 1979. During 1980–2012, he worked at Yokohama National University, Tokyo Metropolitan University, and the Institute for Molecular Science as a Professor. From 2012, he started to work at Fukui Institute for Fundamental Chemistry, Kyoto University, as a Senior Research Fellow. He has great interest in developing new molecules and reactions through close interplay between theoretical predictions and experimental tests. He received The Commendation for Science and Technology (Research Category) from The Ministry of Education, Culture, Sports, Science and Technology of Japan (2011) and The Chemical Society of Japan Award (2013).

FOOTNOTES

*E-mail addresses: lux@hust.edu.cn; akasaka@tara.tsukuba.ac.jp.
The authors declare no competing financial interest.

REFERENCES

1 Kroto, H. W.; Heath, J. R.; O'Brien, S. C.; Curl, R. F.; Smalley, R. E. C_{60}-Buckminsterfullerene. *Nature* **1985**, *318*, 162–163.
2 Akasaka, T.; Wudl, F.; Nagase, S. *Chemistry of Nanocarbons*; John Wiley & Sons Ltd.: Chichester, 2010.
3 Hirsch, A.; Brettreich, M. *Fullerenes – Chemistry and Reactions*; Wiley-VCH: Weinheim, Germany, 2005.
4 Vostrowsky, O.; Hirsch, A. Heterofullerenes. *Chem. Rev.* **2006**, *106*, 5191–5207.
5 Akasaka, T.; Nagase, S. *Endofullerenes: A New Family of Carbon Clusters*; Kluwer: Dordrecht, the Netherlands, 2002.
6 Lu, X.; Feng, L.; Akasaka, T.; Nagase, S. Current status and future developments of endohedral metallofullerenes. *Chem. Soc. Rev.* **2012**, *41*, 7723–7760.
7 Kratschmer, W.; Lamb, L. D.; Fostiropoulos, K.; Huffman, D. R. Solid C_{60} - a new form of carbon. *Nature* **1990**, *347*, 354–358.
8 Chaur, M. N.; Melin, F.; Ortiz, A. L.; Echegoyen, L. Chemical, electrochemical, and structural properties of endohedral metallofullerenes. *Angew. Chem., Int. Ed.* **2009**, *48*, 7514–7538.
9 Stevenson, S.; Rice, G.; Glass, T.; Harich, K.; Cromer, F.; Jordan, M. R.; Craft, J.; Hadju, E.; Bible, R.; Olmstead, M. M.; Maitra, K.; Fisher, A. J.; Balch, A. L.; Dorn, H. C. Small-bandgap endohedral metallofullerenes in high yield and purity. *Nature* **1999**, *401*, 55–57.
10 Rodriguez-Fortea, A.; Balch, A. L.; Poblet, J. M. Endohedral metallofullerenes: A unique host–guest association. *Chem. Soc. Rev.* **2011**, *40*, 3551–3563.
11 Takata, M.; Umeda, B.; Nishibori, E.; Sakata, M.; Saito, Y.; Ohno, M.; Shinohara, H. Confirmation by X-ray diffraction of the endohedral character of the metallofullerene Y@C_{82}. *Nature* **1995**, *377*, 46–49.
12 Wang, C. R.; Kai, T.; Tomiyama, T.; Yoshida, T.; Kobayashi, Y.; Nishibori, E.; Takata, M.; Sakata, M.; Shinohara, H. A scandium carbide endohedral metallofullerene: Sc_2C_2@C_{84}. *Angew. Chem., Int. Ed.* **2001**, *40*, 397–399.
13 Akasaka, T.; Nagase, S.; Kobayashi, K.; Walchli, M.; Yamamoto, K.; Funasaka, H.; Kako, M.; Hoshino, T.; Erata, T. ^{13}C and ^{139}La NMR studies of La_2@C_{80}: First evidence for circular motion of metal atoms in endohedral dimetallofullerenes. *Angew. Chem., Int. Ed.* **1997**, *36*, 1643–1645.
14 Popov, A. A.; Dunsch, L. Structure, stability, and cluster–cage interactions in nitride clusterfullerenes M_3N@C_{2n} (M = Sc, Y; 2n = 68–98): A density functional theory study *J. Am. Chem. Soc.* **2007**, *129*, 11835–11849.
15 Hachiya, M.; Nikawa, H.; Mizorogi, N.; Tsuchiya, T.; Lu, X.; Nagase, S.; Akasaka, T. Exceptional chemical properties of Sc@C_{2v}(9)-C_{82} probed with adamantylidene carbene *J. Am. Chem. Soc.* **2012**, *134*, 15550–15555.
16 Yamazaki, Y.; Nakajima, K.; Wakahara, T.; Tsuchiya, T.; Ishitsuka, M. O.; Maeda, Y.; Akasaka, T.; Waelchli, M.; Mizorogi, N.; Nagase, S. Observation of ^{13}C NMR chemical shifts of metal carbides encapsulated in fullerenes: Sc_2C_2@C_{82}, Sc_2C_2@C_{84}, and Sc_3C_2@C_{80}. *Angew. Chem., Int. Ed.* **2008**, *47*, 7905–7908.
17 Kurihara, H.; Lu, X.; Iiduka, Y.; Nikawa, H.; Hachiya, M.; Mizorogi, N.; Slanina, Z.; Tsuchiya, T.; Nagase, S.; Akasaka, T. X-ray structures of Sc_2C_2@C_{2n} (n = 40–42): In-depth understanding of the core–shell interplay in carbide cluster metallofullerenes. *Inorg. Chem.* **2012**, *51*, 746–750.
18 Inakuma, M.; Yamamoto, E.; Kai, T.; Wang, C. R.; Tomiyama, T.; Shinohara, H.; Dennis, T. J. S.; Hulman, M.; Krause, M.; Kuzmany, H. Structural and electronic properties of isomers of Sc_2@C_{84}(I, II, III): ^{13}C NMR and IR/Raman spectroscopic studies. *J. Phys. Chem. B* **2000**, *104*, 5072–5077.
19 Iiduka, Y.; Wakahara, T.; Nakajima, K.; Tsuchiya, T.; Nakahodo, T.; Maeda, Y.; Akasaka, T.; Mizorogi, N.; Nagase, S. ^{13}C NMR spectroscopic study of scandium dimetallofullerene, Sc_2@C_{84} vs. Sc_2C_2@C_{82}. *Chem. Commun.* **2006**, 2057–2059.
20 Lu, X.; Nakajima, K.; Iiduka, Y.; Nikawa, H.; Mizorogi, N.; Slanina, Z.; Tsuchiya, T.; Nagase, S.; Akasaka, T. Structural elucidation and regioselective functionalization of an unexplored carbide cluster metallofullerene Sc_2C_2@C_s(6)-C_{82}. *J. Am. Chem. Soc.* **2011**, *133*, 19553–19558.
21 Lu, X.; Nakajima, K.; Iiduka, Y.; Nikawa, H.; Tsuchiya, T.; Mizorogi, N.; Slanina, Z.; Nagase, S.; Akasaka, T. The long-believed Sc_2@C_{2v}(17)-C_{84} is actually Sc_2C_2@C_{2v}(9)-C_{82}: Unambiguous structure assignment and chemical functionalization. *Angew. Chem., Int. Ed.* **2012**, *51*, 5889–5892.

22 Suenaga, K.; Okazaki, T.; Wang, C. R.; Bandow, S.; Shinohara, H.; Iijima, S. Direct imaging of $Sc_2@C_{84}$ molecules encapsulated inside single-wall carbon nanotubes by high resolution electron microscopy with atomic sensitivity. *Phys. Rev. Lett.* **2003**, *90*, No. 055506.

23 Takata, M.; Nishibori, E.; Sakata, M.; Inakuma, M.; Yamamoto, E.; Shinohara, H. Triangle scandium cluster imprisoned in a fullerene cage. *Phys. Rev. Lett.* **1999**, *83*, 2214–2217.

24 Iiduka, Y.; Wakahara, T.; Nakahodo, T.; Tsuchiya, T.; Sakuraba, A.; Maeda, Y.; Akasaka, T.; Yoza, K.; Horn, E.; Kato, T.; Liu, M. T. H.; Mizorogi, N.; Kobayashi, K.; Nagase, S. Structural determination of metallofullerene Sc_3C_{82} revisited: A surprising finding. *J. Am. Chem. Soc.* **2005**, *127*, 12500–12501.

25 Wang, T. S.; Chen, N.; Xiang, J. F.; Li, B.; Wu, J. Y.; Xu, W.; Jiang, L.; Tan, K.; Shu, C. Y.; Lu, X.; Wang, C. R. Russian-doll-type metal carbide endofullerene: Synthesis, isolation, and characterization of $Sc_4C_2@C_{80}$. *J. Am. Chem. Soc.* **2009**, *131*, 16646–16647.

26 Kurihara, H.; Lu, X.; Iiduka, Y.; Mizorogi, N.; Slanina, Z.; Tsuchiya, T.; Akasaka, T.; Nagase, S. $Sc_2C_2@C_{80}$ rather than $Sc_2@C_{82}$: Templated formation of unexpected $C_{2v}(5)$-C_{80} and temperature-dependent dynamic motion of internal Sc_2C_2 cluster. *J. Am. Chem. Soc.* **2011**, *133*, 2382–2385.

27 Kurihara, H.; Lu, X.; Iiduka, Y.; Nikawa, H.; Mizorogi, N.; Slanina, Z.; Tsuchiya, T.; Nagase, S.; Akasaka, T. Chemical understanding of carbide cluster metallofullerenes: A case study on $Sc_2C_2@C_{2v}(5)$-C_{80} with complete X-ray crystallographic characterizations. *J. Am. Chem. Soc.* **2012**, *134*, 3139–3144.

28 Shi, Z. Q.; Wu, X.; Wang, C. R.; Lu, X.; Shinohara, H. Isolation and characterization of $Sc_2C_2@C_{68}$: A metal−carbide endofullerene with a non-IPR carbon cage. *Angew. Chem., Int. Ed.* **2006**, *45*, 2107–2111.

29 Zheng, H.; Zhao, X.; Wang, W. W.; Yang, T.; Nagase, S. $Sc_2@C_{70}$ rather than $Sc_2C_2@C_{68}$: Density functional theory characterization of metallofullerene Sc_2C_{70}. *J. Chem. Phys.* **2012**, *137*, No. 014308.

30 Iiduka, Y.; Wakahara, T.; Nakajima, K.; Nakahodo, T.; Tsuchiya, T.; Maeda, Y.; Akasaka, T.; Yoza, K.; Liu, M. T. H.; Mizorogi, N.; Nagase, S. Experimental and theoretical studies of the scandium carbide endohedral metallofullerene $Sc_2C_2@C_{82}$ and its carbene derivative. *Angew. Chem., Int. Ed.* **2007**, *46*, 5562–5564.

31 Tan, K.; Lu, X. Ti_2C_{80} is more likely a titanium carbide endohedral metallofullerene $Ti_2C_2@C_{78}$. *Chem. Commun.* **2005**, 4444–4446.

32 Inoue, T.; Tomiyama, T.; Sugai, T.; Okazaki, T.; Suematsu, T.; Fujii, N.; Utsumi, H.; Nojima, K.; Shinohara, H. Trapping a C_2 radical in endohedral metallofullerenes: Synthesis and structures of $Y_2C_2@C_{82}$ (Isomers I, II, and III). *J. Phys. Chem. B* **2004**, *108*, 7573–7579.

33 Zhang, J.; Fuhrer, T.; Fu, W. J.; Ge, Z.; Bearden, D. W.; Dallas, J.; Duchamp, J.; Walker, K.; Champion, H.; Azurmendi; Harich, K.; Dorn, H. C. Nanoscale fullerene compression of an yttrium carbide cluster. *J. Am. Chem. Soc.* **2012**, *134*, 8487–8493.

34 Xu, W.; Wang, T.-S.; Wu, J.-Y.; Ma, Y.-H.; Zheng, J.-P.; Li, H.; Wang, B.; Jiang, L.; Shu, C.-Y.; Wang, C.-R. Entrapped planar trimetallic carbide in a fullerene cage: Synthesis, isolation and spectroscopic studies of $Lu_3C_2@C_{88}$. *J. Phys. Chem. C* **2011**, *115*, 402–405.

35 Ito, Y.; Okazaki, T.; Okubo, S.; Akachi, M.; Ohno, Y.; Mizutani, T.; Nakamura, T.; Kitaura, R.; Sugai, T.; Shinohara, H. Enhanced 1520 nm photoluminescence from Er^{3+} ions in di-erbium-carbide metallofullerenes $Er_2C_2@C_{82}$ (isomers I, II, and III). *ACS Nano* **2007**, *1*, 456–462.

36 Yang, H.; Lu, C.; Liu, Z.; Jin, H.; Che, Y.; Olmstead, M. M.; Balch, A. L. Detection of a family of gadolinium-containing endohedral fullerenes and the isolation and crystallographic characterization of one member as a metal−carbide encapsulated inside a large fullerene cage. *J. Am. Chem. Soc.* **2008**, *130*, 17296–17300.

37 Yamada, M.; Feng, L.; Wakahara, T.; Tsuchiya, T.; Maeda, Y.; Lian, Y. F.; Kako, M.; Akasaka, T.; Kato, T.; Kobayashi, K.; Nagase, S. Synthesis and characterization of exohedrally silylated $M@C_{82}$ (M = Y and La). *J. Phys. Chem. B* **2005**, *109*, 6049–6051.

38 Lu, X.; Akasaka, T.; Nagase, S. Chemistry of endohedral metallofullerenes: The role of metals. *Chem. Commun.* **2011**, *47*, 5942–5957.

39 Lu, X.; Nikawa, H.; Feng, L.; Tsuchiya, T.; Maeda, Y.; Akasaka, T.; Mizorogi, N.; Slanina, Z.; Nagase, S. Location of the yttrium atom in $Y@C_{82}$ and its influence on the reactivity of cage carbons. *J. Am. Chem. Soc.* **2009**, *131*, 12066–12067.

40 Wang, T. S.; Wu, J. Y.; Xu, W.; Xiang, J. F.; Lu, X.; Li, B.; Jiang, L.; Shu, C. Y.; Wang, C. R. Spin divergence induced by exohedral modification: ESR study of $Sc_3C_2@C_{80}$ fulleropyrrolidine. *Angew. Chem., Int. Ed.* **2010**, *49*, 1786–1789.

41 Kurihara, H.; Iiduka, Y.; Rubin, Y.; Waelchli, M.; Mizorogi, N.; Slanina, Z.; Tsuchiya, T.; Nagase, S.; Akasaka, T. Unexpected formation of a $Sc_3C_2@C_{80}$ bisfulleroid derivative. *J. Am. Chem. Soc.* **2012**, *134*, 4092–4095.

42 Chen, C. H.; Yeh, W. Y.; Liu, Y. H.; Lee, G. H. $[(\mu\text{-H})_3Re_3(CO)_9(\eta^2,\eta^2,\eta^2\text{-}Sc_2C_2@C_{3v}(8)\text{-}C_{82})]$: Face-capping cluster complex of an endohedral fullerene. *Angew. Chem., Int. Ed.* **2012**, *51*, 13046–13049.

43 Dunk, P. W.; Kaiser, N. K.; Hendrickson, C. L.; Quinn, J. P.; Ewels, C. P.; Nakanishi, Y.; Sasaki, T.; Shinohara, H.; Marshall, A. G.; Kroto, H. W. Closed network growth of fullerenes. *Nat. Commun.* **2012**, *3*, 855.

44 Chaur, M. N.; Melin, F.; Ashby, J.; Elliott, B.; Kumbhar, A.; Rao, A. M.; Echegoyen, L. Lanthanum nitride endohedral fullerenes $La_3N@C_{2n}$ ($43 \leq n \leq 55$): Preferential formation of $La_3N@C_{96}$. *Chem.—Eur. J.* **2008**, *14*, 8213–8219.